Journal of Cardiology (2008) **51**, 179—188

ELSEVIER

JOURNAL of CARDIOLOGY
Official Journal of the Japanese College of Cardiology
www.elsevier.com/locate/jjcc

ORIGINAL ARTICLE

The usefulness of delayed enhancement magnetic resonance imaging for diagnosis and evaluation of cardiac function in patients with cardiac sarcoidosis

Fumitaka Matoh (MD, PhD)[a,*], Hiroshi Satoh (MD, PhD)[b], Katsunori Shiraki (MD)[b], Keiichi Odagiri (MD)[b], Takeji Saitoh (MD)[b], Tsuyoshi Urushida (MD)[b], Hideki Katoh (MD, PhD)[b], Yasuo Takehara (MD, PhD), Harumi Sakahara (MD, PhD)[c], Hideharu Hayashi (MD, PhD)[b]

[a] *Department of Emergency Medicine, Hamamatsu University School of Medicine, 1-20-1 Handayama, Hamamatsu 431-3192, Japan*
[b] *Division of Cardiology, Internal Medicine III, University School of Medicine, Hamamatsu, Japan*
[c] *Department of Radiology, Hamamatsu University School of Medicine, Hamamatsu, Japan*

Received 20 December 2007; accepted 18 March 2008
Available online 24 April 2008

KEYWORDS
Magnetic resonance imaging;
Delayed enhancement;
Sarcoidosis;
Left ventricular function;
Single-photon emission computed tomography

Summary
Objectives: Cardiac involvement is an important prognostic factor in patients with sarcoidosis. We evaluated the usefulness of delayed enhancement MRI (DE-MRI) for diagnosing cardiac sarcoidosis by comparing with nuclear imaging and studying the correlation between DE area and left ventricular (LV) function.
Methods: Twelve patients (male:female 3:9) diagnosed as having sarcoidosis underwent Gd-MRI, myocardial perfusion SPECT (Tl-201, Tc-99m sestamibi), Ga-67 scintigraphy, and/or F-18 FDG-PET.
Results: DE was observed in 5 patients, and was positive in 39 (39%) of 100 LV segments. The corresponding perfusion defects in myocardial perfusion SPECT were undetectable in 14 (36%) segments. DE distributed mainly in mid- to epi-myocardium, and the lack of perfusion defects in myocardial perfusion SPECT was more prominent in less transmural DE segments. Two patients with diffuse DE and 1 case with focal DE exhibited positive cardiac uptake in Ga-67 scintigraphy, and 2 other cases with focal DE showed cardiac uptake in F-18 FDG-PET. In 7 patients without DE, there were no significant findings in nuclear imaging. Both LV end-diastolic and end-systolic volume were positively and LV ejection fraction was negatively correlated with the extent of

* Corresponding author. Tel.: +81 53 435 2759; fax: +81 53 435 2796.
E-mail address: wbs01352@mail.wbs.ne.jp (F. Matoh).

0914-5087/$ — see front matter
doi:10.1016/j.jjcc.2008.03.002

DE area. Four patients treated with corticosteroid showed improvement in nuclear imaging and slight decreases in DE area but no recovery in LV function.
Conclusions: DE-MRI is useful to diagnose the cardiac involvement of sarcoidosis and to evaluate cardiac function. It is likely that the distribution of DE in mid- to epimyocardium is the characteristic of cardiac sarcoidosis, and the larger DE area may be correlated with poor LV function.

Introduction

Sarcoidosis is a multi-system disorder of unknown etiology. Although the organ most frequently involved is lung, all parts of the body can be affected. Cardiac involvement is symptomatic in only 5% of patients with sarcoidosis, whereas sudden death resulting from ventricular tachyarrhythmias or conduction block accounts for 30—65% of death caused by sarcoidosis. Actually, the cardiac involvement is apparent at postmortem in 20—50% of patients [1—4]. In Japan, more patients have cardiac lesions compared with those in the western countries, and 47—78% of patients die of cardiac events [5,6]. It has been reported that the early initiation of corticosteroid therapy improves left ventricular function and prevents malignant arrhythmias [7,8].

Endomyocardial biopsy may be essential to diagnose cardiac sarcoidosis. However, it is invasive and sometimes false negative because of inhomogeneous myocardial invasion of sarcoidosis lesion. Although Tl-201 and Ga-67 scintigraphy have been used to detect cardiac involvement in patients with sarcoidosis [9—11], both methods are relatively low in spatial resolution. Recent studies have revealed that F-18 FDG-PET may be useful for the detection of cardiac sarcoidosis [12,13]. However, this method is performed only in limited facilities and requires a large amount of cost.

Myocardial magnetic resonance imaging (MRI) is non-invasive, does not expose the patient to ionizing radiation, and is excellent for spatial resolution. Delayed enhancement (DE)-MRI has been shown useful to detect small and focal myocardial abnormality [14—16]. Several reports have shown that the distribution of DE in cardiac sarcoidosis may be different from that in myocardial infarction [17—25]. However, it is still unclear whether DE-MRI is actually useful to detect cardiac sarcoidosis, whether the extent of DE is associated with cardiac dysfunction, and whether DE disappears by corticosteroid therapy.

This study was planned to compare the usefulness of DE-MRI for the detection of cardiac sarcoidosis with other nuclear imaging modalities, to examine the relationship between the extent of DE and left ventricular function, and to evaluate the effects of corticosteroid therapy.

Patients and methods

Patients

We studied 12 patients (3 men, 9 women; 58.7 ± 11.3 years old) with sarcoidosis who underwent cardiac DE-MRI from May 2003 to January 2006. The diagnosis of sarcoidosis was provided histologically or according to Proposal by the Specific Diffuse Pulmonary Disease Research Group, Sarcoidosis Division by the Japanese Ministry of Health and Welfare [26]. The patient characteristics are shown in Table 1. Ten of 12 patients were diagnosed as sarcoidosis by eye lesions or bilateral hilar lymphadenopathy (BHL), and 3 patients were by histology in scalene nodes (cases 1 and 5) or a gastrocnemial muscle (case 11). The cardiac involvement of sarcoidosis was also evaluated according to the criteria of the Japanese Society of Sarcoidosis and other Granulomatous Disorders [27]. As shown in Table 1, 8, 10 and 3 patients also underwent myocardial perfusion single-photon emission computed tomography (SPECT) (7 cases with Tl-201 and 1 case with Tc-99m sestamibi), whole-body Ga-67 planar imaging, and F-18 FDG-PET, respectively. This study protocol was in accordance with the Declaration of Helsinki and approved by the institutional review board (Hamamatsu University School of Medicine, Hamamatsu, Japan), and all patients gave informed consent.

MRI protocol

All the 12 patients underwent electrocardiogram-gated MRI. Imaging was performed on a 1.5 T MR system (Signa Infinity Twinspeed, GE Medical Systems, Waukesha, Wis) with a gradient system performance of maximum amplitude of 40 mT/m and slew time of 150 T/m/s. An 8-element phased array cardiac coil was used in all studies. Typi-

Table 1 Patient characteristics and findings in DE-MRI and nuclear imaging

Patient no.	Sex	Age (years)	Symptom	Extra-cardiac lesions	ECG findings	DE pattern	LVEF with Cine MRI (%)	ACE (IU/L)	SPECT	Ga-67	F-18 FDG
DE(+)											
1	F	67	Dyspnea	SN	RBBB, LAD, abnormal Q	Diffuse	11	3.9	(+)	(+)	N.A.
2	F	55	Dyspnea	BHL	Abnormal Q	Diffuse	22	14.9	(+)	(+)	N.A.
3	F	56	Blurred vision	Eye, skin, BHL	Normal	Focal	66	15.8	(−)	(−)	(+)
4	M	64	Blurred vision, dyspnea	Eye	Normal	Focal	58	8.9	(−)	(−)	(+)
5	F	41	Palpitation	Eye, lung, BHL, SN	Normal	Focal	41	17.1	(−)*	(+)	N.A.
DE(−)											
6	F	65	Blurred vision	Eye, BHL	Negative T		67	8.7	N.A.	N.A.	N.A.
7	F	67	(−)	Eye	Normal		70	N.A.	N.A.	N.A.	N.A.
8	M	41	(−)	BHL	Normal		64	16.7	(−)	(−)	N.A.
9	F	77	Blurred vision	Eye	Normal		75	35.1	(−)	(−)	N.A.
10	M	57	(−)	Eye, BHL	Normal		55	11.9	(−)	(−)	N.A.
11	F	67	(−)	Muscle	Normal		70	22.6	N.A.	(−)	(−)
12	F	47	(−)	Lung, BHL, CNS	Normal		63	23.0	N.A.	(−)	N.A.

ACE: angiotensin-converting enzyme, DE: delayed enhancement, SPECT: defects in thallium-201 or technesium-99m sestamibi* SPECT, Ga-67: uptake in gallium-67 scintigraphy, F-18 FDG: uptake in fluorosis-18 fluorodeoxy glucose PET, SN: scalene node, BHL: bilateral hilar lymphadenopathy, CNS; central nervous system, RBBB: right bundle branch block, LAD: left axis deviation, N.A.: not available.

cally, 3 planes such as short axis, sagittal long axis and 4-chamber view were obtained for 2D FIESTA cine images and delayed myocardial enhancement images. 2D FIESTA cine images were based on the steady state free precession (SSFP) sequence and delayed myocardial enhancement imaging was based on the inversion recovery prepared fast gradient echo (IR-FGRE) sequence. The 6—9 slices were used to cover whole heart. The slice thickness/gap was typically 10 mm/0 mm. The matrix was 192×192 for 2D FIESTA cine, and 256×160 for IR-FGRE. The trigger delay for IR-FGRE was 300 ms; however, for the patients with tachycardia, system-dependent trigger delay time was selected, which was shorter than 300 ms. The readout data line for IR-FGRE was 160 each, where 24 data lines were acquired per segment. FOV was 34 cm for both sequences. Sixteen data lines were acquired per each segment, and 16 phases were acquired for 2D FIESTA cine sequences. Shortest TR and TE were selected; however, the values were not exactly the same for each study, because they were related to the orientation of scanning plane and slice thickness. Sequence parameters were (2D FIESTA and IR-FGRE, respectively), flip angle: 45° and 20°; readout bandwidth: 125 kHz and 31.25 kHz. Breath-hold cine MR images were obtained in contiguous short-axis planes from the apex to the base of the heart with the patient in a resting state. After the 2D FIESTA cine images were acquired, 0.2 mmol/kg of contrast material (Gd-DTPA-BMA, Daiichi Pharma., Tokyo) was injected, and after a 15 min delay, delayed myocardial enhancement images were acquired. Thus, optimum TIs for the IR-FSPGR were measured right before the DE, which were between 200 ms and 240 ms. This process in search of optimum contrast was concluded within three minutes.

Nuclear imaging protocol

The myocardial perfusion SPECT was performed using Tl-201 or Tc-99m sestamibi (MIBI). The SPECT images were obtained with a triple-head gamma camera (PRISM 3000, Picker International, USA) and a dual-head gamma camera (Millennium VG, GE Yokokawa Co., Japan) equipped with low energy high-resolution collimators, respectively. The detailed protocols for SPECT were described elsewhere [28].

Ga-67 scintigraphy was performed using 111 MBq Ga-67 citrate and a large field of view gamma camera (Prism 2000, Picker International, USA or Millennium VG, GE Yokokawa Co., Japan) with medium-energy and general purpose collimator. Twenty percent windows were placed symmetrically around each of the three main photopeaks of Ga-67 (93 keV, 184 keV and 300 keV). Whole body images (anterior and posterior view images) were taken at a speed of 8—10 cm/min on 72 h after injection.

F-18 FDG-PET was performed using a SHR 22000 PET scanner (Hamamatsu Photonics, K.K., Hamamatsu, Japan) [29]. The SHR 22000 scanner permits simultaneous acquisition of 63 transverse planes of 3.6-mm thickness encompassing a 23.0-cm axial field of view. The patients fasted for at least 5 h were asked to lie supine on the imaging bed of the PET camera with both arms extended out of the field of view. Initial transmission scanning of the region of interest (ROI) was performed for 15 min with a germanium-68 ring source. Acquired data were later used for attenuation correction in image reconstruction. Serum glucose levels measured before each PET scanning session were normal (72—118 mg/dl).

Analysis of MRI and nuclear images

Two experienced cardiovascular radiologists interpreted all initial and follow-up MRIs and nuclear images without knowledge of clinical findings. Left ventricular end-diastolic volume (LVEDV), end-systolic volume (LVESV), and ejection fraction (LVEF) were acquired from the 2D FIESTA cine images in short axis view. Regional analyses of DE-MRI and Tl-201 or Tc-sestamibi SPECT were performed using the 20-segments model [30]. The segmental transmural distribution of DE was also determined visually as endo-, mid-, and epi-myocardium. To estimate DE quantitatively, the DE area was traced manually and the percentage against total LV area was calculated (%DEA). The intra- and inter-observer variability for measurement of %DEA were acceptable (intra-observer: $r = 0.91$, $p < 0.01$, inter-observer: $r = 0.84$, $p < 0.01$).

Statistical analyses

Data were expressed as means ± standard deviation (S.D.). The Wilcoxon rank-sum test for unpaired data was used to examine differences between groups. Correlation between the extent of DE (%DEA) and LV function was assessed by Pearson's correlation coefficient (r). Differences were considered significant when $p < 0.05$.

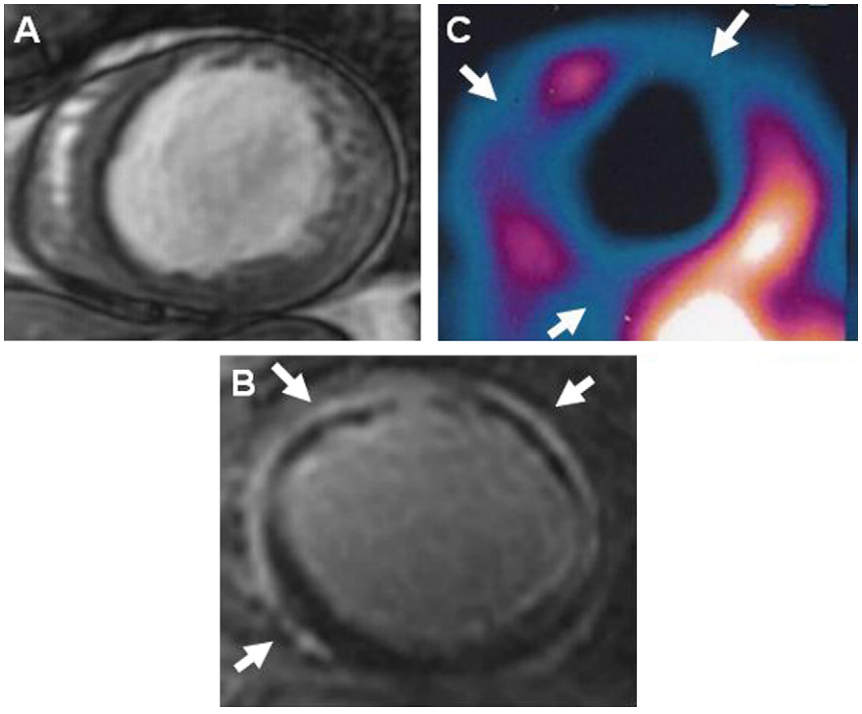

Figure 1 A representative case with diffuse type delayed enhancement (DE). (A) Cine MRI. (B) DE-MRI. The area of DE mainly distributed in mid- to epi-myocardium (arrows). (C) The corresponding image of Tl-201 SPECT exhibited focal perfusion defects only in anterior, antero-septal and inferior segments (arrows).

Results

Patient characteristics

Table 1 summarizes the clinical characteristics of the patients and the findings in myocardial imaging. The delayed myocardial enhancement (DE) was observed in 5 of 12 patients. In the 5 patients with DE, 4 cases complained of dyspnea or palpitation, whereas there was no case who had cardiac symptoms in the 7 patients without DE. The pattern of DE in the 5 positive cases was clearly discriminated as diffuse or focal enhancement. In focal type DE, the area of DE was less than 50% in each slice of LV. In patients with diffuse type DE, case 1 showed right bundle branch block, left axis deviation and abnormal Q waves in V5, V6 leads, and case 2 had abnormal Q waves in I, II, aVF, V3—V6 leads. In patients with focal type DE and in those without DE, only case 6 exhibited negative T waves in V3—V6 leads. Thus, none of the patients with focal type DE or without DE satisfied the criteria of cardiac sarcoidosis.

The high angiotensin-converting enzyme (ACE) activity was seen only in case 9. LVEF obtained with cine MRI were $39.6 \pm 23.3\%$ in patients with DE ($n = 5$) and $65.6 \pm 2.8\%$ ($n = 6$) in patients without DE ($p < 0.05$ by Wilcoxon rank-sum test).

The pattern of DE

In 2 cases with diffuse type DE, the enhancement spread to almost all slices of LV, and the values of total %DEA were 18.4% and 35%. Fig. 1 demonstrates a typical case of diffuse type DE (case 2). Notably, the area of DE mainly distributed in mid- to epi-myocardium. The Tl-201 SPECT image exhibited only focal perfusion defects in anterior, antero-septal and inferior segments. On the other hand, in 3 cases with focal DE, the values of %DEA were 6.7%, 6.8% and 16.3%. Fig. 2 expresses a typical case of focal type DE (case 4). The DE existed only in the mid-ventricle of antero-lateral segment of LV (B), whereas the Tl-201 SPECT image showed no perfusion defect (C).

Comparison with nuclear cardiac imaging

As shown in Table 1, 2 patients with diffuse type DE exhibited defects in myocardial Tl-201 SPECT and positive cardiac uptake in Ga-67 scintigraphy. Three patients with focal type DE showed no defects in myocardial perfusion SPECT, but had cardiac uptake in Ga-67 scintigraphy (case 5) or in F-18 FDG-PET (cases 3 and 4). In 7 patients without DE, available cases showed no defects in myocardial Tl-201

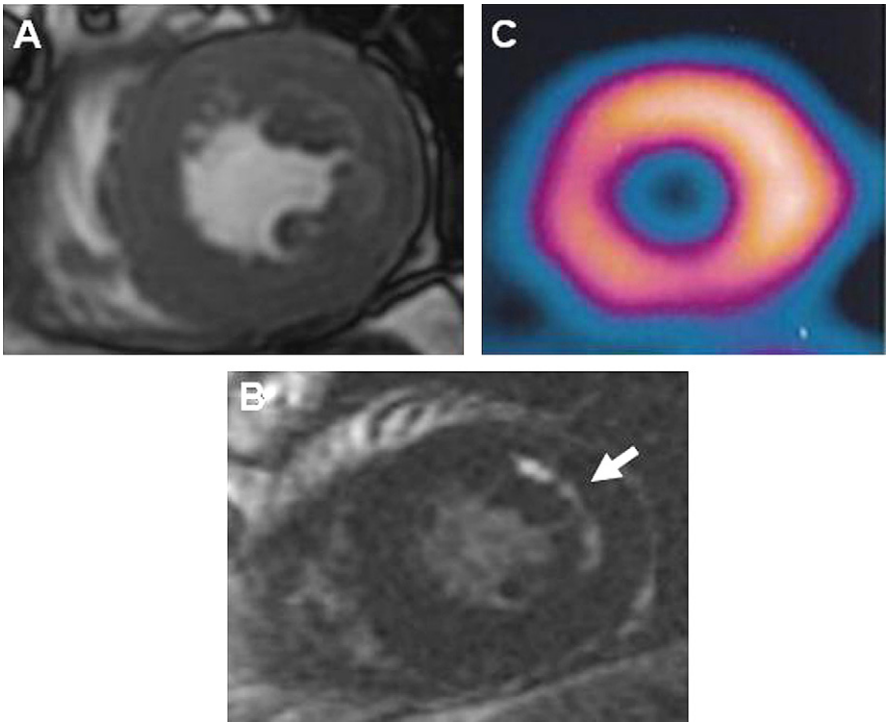

Figure 2 A representative case with focal type DE. (A) Cine MRI. (B) DE-MRI. The area of DE existed only in the mid-ventricle of antero-lateral segment of LV (arrow). (C) The corresponding image of Tl-201 SPECT showed no perfusion defect.

SPECT, no uptake in Ga-67 scintigraphy or in F-18 FDG-PET.

Fig. 3 demonstrates the numbers of segments that showed DE and defects in myocardial perfusion SPECT (in parentheses) in 5 patients with DE. By the regional analysis using 20 segments model [30], the total of 100 LV segments in the 5 patients were analyzed. Among the 100 LV segments, DE was observed in 39 (39%) segments. The DE spread to all the LV segments, and there was no tendency in the distribution of DE. In 14 of the 39 segments (36%), the corresponding perfusion defects in myocardial perfusion SPECT were undetectable. Fig. 4 shows the relationship between intramural distribution of DE (open columns) and perfusion defects in myocardial perfusion SPECT (filled columns). It was evident that DE distributed in endo-myocardium to trans-mural myocardium, but mainly in mid- to epi-myocardium. All the segments with transmural DE showed the perfusion defects in myocardial perfusion SPECT. The lack of perfusion defects in myocardial perfusion SPECT was more prominent in less transmural DE segments.

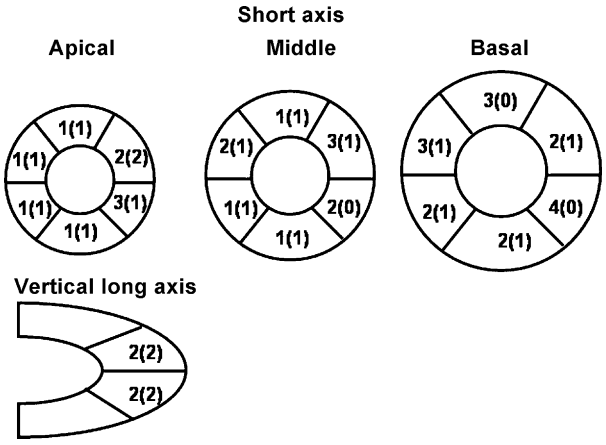

Figure 3 The numbers of segments which showed DE and defects in Tl-201 SPECT (parentheses) in patients with DE. Among the 100 LV segments in 5 patients, DE was observed in 39 (39%) segments. The DE spread to all the LV segments, and there was no tendency in the distribution of DE. The numbers in parentheses indicate those with perfusion defect in myocardial perfusion SPECT (Tl-201 or Tc-99m sestamibi). In 14 of the 39 DE segments (36%), the corresponding perfusion defects SPECT were undetectable.

Relationship between %DEA and LV function

Fig. 5 shows the relationship between the extent of DE (%DEA) and LV function. The values are derived from patients without DE (open circles), those with focal type DE (closed circles), and those with diffuse type DE (closed triangles), respectively. Both LVEDV and LVESV were positively correlated with

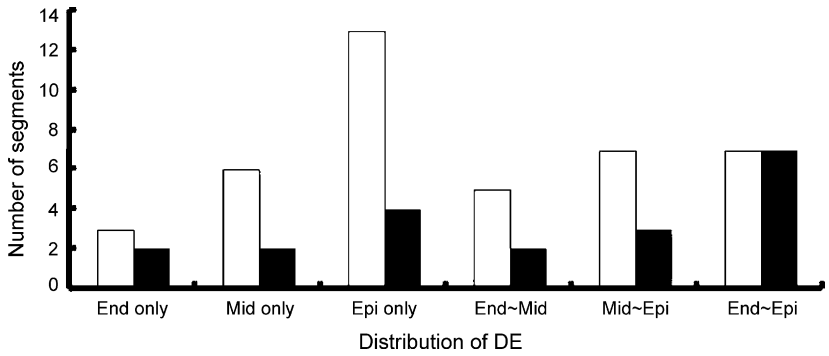

Figure 4 The relationship between intramural distribution of DE (open columns) and corresponding perfusion defects in myocardial perfusion SPECT (filled columns). DE distributed in endo-myocardium to transmural myocardium, but mainly in mid- to epi-myocardium. Additionally, the lack of perfusion defects in myocardial perfusion SPECT was more prominent in less transmural DE segments. The segmental transmural distribution of DE was determined visually in DE-MRI. Endo, Mid, Epi: Endo-, mid-, epi-myocardium.

%DEA ($r = 0.88$, and $r = 0.88$, $p < 0.01$). Conversely, LVEF was negatively correlated with %DEA ($r = 0.85$, $p < 0.01$).

Corticosteroid therapy and DE

In 4 patients (cases 1, 3, 4 and 5) with DE, the corticosteroid therapy was applied for 2—12 months. In a patient with diffuse type DE (case 1), the decrease in %DEA and the increase in LVEF were small (%DEA: 18.4—15.1%, LVEF: 11—20%), but both the defects in myocardial Tl-201 imaging and cardiac uptake in Ga-67 scintigraphy disappeared. In 3 patients with focal type DE (cases 3, 4 and 5), %DEA slightly decreased in 2 cases (6.7—7.7%, 7.7—5.7% and 16.3—13.7%), but LVEF did not change (67—66%, 53—51% and 41—41%). However, the cardiac uptake in F-18 FDG-PET or Ga-67 scintigraphy apparently decreased in these cases.

Discussion

In this study, 5 of 12 (42%) patients with sarcoidosis showed DE in cardiac DE-MRI, and the pattern of DE was clearly discriminated as diffuse or focal enhancement. The DE area mainly distributed in mid- to epi-myocardium, and the %DEA was significantly correlated with LV function. DE-MRI is, therefore, useful to diagnose the cardiac involvement of sarcoidosis and to evaluate cardiac function.

The usefulness of DE to diagnose cardiac involvement of sarcoidosis

Endomyocardial biopsy has been the only available method to diagnose cardiac involvement of sarcoidosis [31,32]. Several nuclear imaging modalities such as Tl-201 and Ga-67 scintigraphy have also been used to detect cardiac involvement in patients with sarcoidosis [9—11]. In the present study, no patients with DE were proven to have sarcoido-

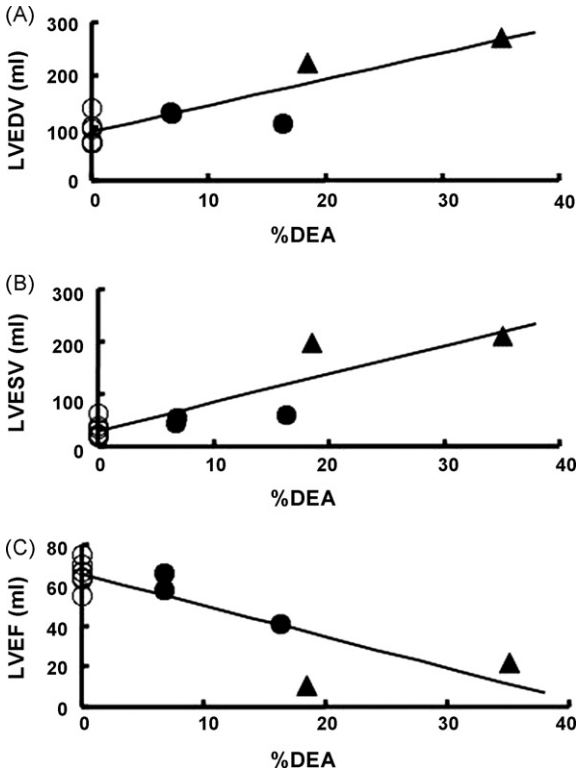

Figure 5 Relationship between %DEA and LVEDV (A), LVESV (B) and LVEF (C). The values are derived from patients without DE (open circles), those with focal type DE (closed circles), and those with diffuse type DE (closed triangles), respectively. Both LVEDV and LVESV were positively correlated with %DEA ($r = 0.88$, and $r = 0.88$, $p < 0.01$). Conversely, LVEF was negatively correlated with %DEA ($r = 0.85$, $p < 0.01$).

sis lesion by endomyocardial biopsy. The 2 patients with diffuse type DE exhibited defects in myocardial Tl-201 imaging and positive cardiac uptake in Ga-67 scintigraphy. In the 3 patients with focal type DE, there were no defects in myocardial perfusion SPECT, but F-18 FDG-PET showed positive cardiac uptake in 2 cases and Ga-67 scintigraphy was positive in 1 case. However, according to the criteria proposed by the Japanese Society of Sarcoidosis and other Granulomatous Disorders [27], none of the patients with focal type DE were diagnosed as cardiac sarcoidosis.

DE in MRI relies on the delivery of intravenous gadolinium chelate to the myocardium, which is a biologically inert tracer that freely distributes in extra-cellular space but does not cross the intact cell membrane. Due to a combination of increased extra-cellular volume and slower washout kinetics, there is a relative accumulation of gadolinium in areas of damaged myocardium in the late washout phase [33].

It has been reported that cardiac MRI shows DE in patients with cardiac sarcoidosis [17—25]. Shimada et al. reported a case of cardiac sarcoidosis in which Tl-201 image was normal but DE-MRI indicated focal type DE in LV [19]. Although several reports have shown that the distribution of DE in cardiac sarcoidosis is different from that in myocardial infarction or hypertrophic cardiomyopathy [14,24,34], there are few detailed studies examining the distribution of DE in LV, and comparing it with the findings in nuclear imaging. In a few reports concerning the pattern of DE, both focal and diffuse types of DE were demonstrated [17—25]. Smedema et al. reported that cardiac MRI revealed DE in 19 of 58 patients with sarcoidosis, mostly involving basal and lateral segments [25]. They also indicated that Tl-201 scintigraphy was normal in 8 of the 19 patients. Their findings are similar to our results, but have not indicated whether DE distributes in endo-myocardium or in mid- to epi-myocardium. Tadamura et al. reported that the transmural extent of DE was related to the defect score in 201-Tl SPECT and to wall motion abnormality [24]. In the present study, the area of DE distributed mainly in mid- to epi-myocardium in all the 5 cases.

In addition, the pattern of DE was clearly discriminated as diffuse or focal enhancement. In 2 cases with diffuse type DE, the enhancement spreads to almost all the slices of LV, and the values of total %DEA were 18.4% and 35%. On the other hand, in the 3 cases with focal type DE, the values of %DEA were 6.7%, 6.8% and 16.3%. The reason for the specific distribution of DE is unknown, but the distribution of DE was obviously discordant with coronary circulation. In lung, the peri-lymphatic progression of sarcoid lesions was reported [35]. An attention should be paid to estimate DE-MRI, since DE-MRI in hypertrophic cardiomyopathy sometimes demonstrates similar distribution pattern of DE [16,34]. We conclude that DE-MRI may be excellent to detect focal involvement of sarcoidosis in which the 12-lead ECG or other imaging modalities showed no abnormal findings.

DE and cardiac function

The extent of DE has been related to the impairment of LV function in cases with ischemic and in hypertrophic cardiomyopathy [16,34,36]. In those reports, LVEDV and ESV obtained with MRI became higher and EF was lower as the DE area increased. In this study, the %DEA was well correlated with LVEDV, ESV and EF. It is therefore indicated that the extent of DE in cardiac sarcoidosis may also be related to the impairment of LV function, although the pattern of DE was much different from that in ischemic cardiomyopathy. Actually, the 2 cases with diffuse type DE had depressed LV function and exhibited ECG abnormalities (bundle branch block and abnormal Q waves), whereas other cases showed no or only minor ECG changes.

Corticosteroid therapy and DE

Ga-67 scintigraphy and F-18 FDG-PET reflect the activity of inflammation and also the involvement of epithelioid cell granuloma in cardiac tissue. Therefore, these methods have been used for the evaluation of the corticosteroid therapy [37—39]. On the other hand, Tl-201 and Tc-99m MIBI express fibrosis and myocardial degeneration. As mentioned above, DE is due to a combination of increased extra-cellular volume and slower washout kinetics [33]. Therefore, DE can occur not only in fibrous scar tissue but also when the volume of Gd distribution increases. In this study, 4 patients underwent corticosteroid therapy for several months. In 1 case with diffuse type DE, both the defects in myocardial Tl-201 SPECT and cardiac uptake in Ga-67 scintigraphy disappeared. In the 3 patients with focal type DE, the cardiac uptake in Ga-67 scintigraphy or F-18 FDG-PET apparently decreased. However, in those cases, the decreases in %DEA were small or lacking. Since LVEF recovered slightly in the 1 case but did not recover in the other 3 cases, DE may indicate the myocardial damage more specifically compared with nuclear imaging that may reflect inflammation. Since DE is caused by a relative accumulation of gadolinium in areas of expanded extracelluar space [40,41], DE in

cardiac sarcoidosis may mean a combination of fibrosis and interstitial edema. In fact, there are several reports that used DE-MRI for the evaluation of the corticosteroid therapy in cardiac sarcoidosis [19—21,42]. Shimada et al. described that the decrease in DE area by corticosteroid therapy may be due to reduction of the interstitial edema [19]. More recently, Tadamura et al. reported a case in which DE area decreased by corticosteroid therapy, but the wall motion abnormalities did not improve as similar to our findings [42].

Limitations

The first limitation in this study was that the diagnosis of sarcoidosis was provided mainly by eye lesions or by BHL. No patients with DE were proven to have sarcoidosis lesion by endomyocardial biopsy. In the 5 cases with DE, there were no stenotic lesions in coronary arteriography and no history of hypertension, valvular heart diseases and familiar cardiomyopathies. The second limitation was that the examination of nuclear imaging was not performed in all patients. Neither myocardial perfusion SPECT nor Ga-67 scintigraphy was available in 2 cases without DE, and F-18 FDG-PET was examined only in 3 cases. Although the lack of full examination was due to clinical and economical problems of the patients, this limitation prevented detailed comparison between MRI and nuclear imaging modalities. The third limitation was that there was no drastic recovery of LV function by corticosteroid therapy. In the 4 cases treated with corticosteroid therapy, the slight decrease in DE area was seen in 3 cases. Therefore, at the present state, we could not determine whether DE means reversible or irreversible myocardial damage.

Conclusion

DE-MRI is useful to diagnose the cardiac involvement of sarcoidosis lesion and to evaluate cardiac function in patients with sarcoidosis. The distribution of DE in mid- to epi-myocardium may be the characteristics of cardiac sarcoidosis, and the increased DE area was associated with poor LV function. Further investigations are necessary to determine whether DE-MRI is more useful than endomyocardial biopsy or nuclear imaging modalities to diagnose cardiac sarcoidosis and to evaluate the efficacy of corticosteroid therapy.

References

[1] Valantine H, Mckenna WJ, Nihoyannpoulos P, Mitchell A, Foale RA, Davies MJ, et al. Sarcoidosis: a pattern of clinical and morphological presentation. Br Heart J 1987;57:256—63.
[2] Silverman KJ, Hutchins GM, Bulkley BH. Cardiac sarcoid: a clinicopathologic study of 84 unselected patients with systemic sarcoidosis. Circulation 1978;58:1204—11.
[3] Abeler V. Sarcoidosis of the cardiac conducting system. Am Heart J 1979;97:701—7.
[4] Vignaux O, Dhote R, Duboc D, Blanche P, Devaux JY, Weber S, et al. Detection of myocardial involvement in patients with sarcoidosis applying T2-weighted, contrast-enhanced, and cine magnetic resonance imaging: initial results of a prospective study. J Comput Assist Tomogr 2002;26:762—7.
[5] Iwai K, Sekiguti M, Hosoda Y, DeRemee RA, Tazelaar HD, Sharma OP, et al. Racial difference in cardiac sarcoidosis incidence observed at autopsy. Sarcoidosis 1994;11:26—31.
[6] Iwai K, Tachibana T, Takemura T, Matsui Y, Kitaichi M, Kawabata Y. Pathological studies on sarcoidosis autopsy I. epidemiological features of 320 cases in Japan. Acta Pathol Jpn 1993;43:372—6.
[7] Sharma OP. Cardiac and neurologic dysfunction in sarcoidosis. Clin Chest Med 1997;18:813—25.
[8] Yazaki Y, Isobe M, Hiroe M, Morimoto S, Hiramitsu S, Nakano T, et al. Prognostic determinants of long-term survival in Japanese patients with cardiac sarcoidosis treated with predonisone. Am J Cardiol 2001;88:1006—10.
[9] Sharma OP, Maheshwari A, Thaker K. Myocardial sarcoidosis. Chest 1993;103:253—8.
[10] Okayama K, Kurata C, Tawarahara K, Wakabayashi Y, Chida K, Sato A. Diagnostic and prognostic value of myocardial scintigraphy with thallium-201 and gallium-67 in cardiac sarcoidosis. Chest 1995;107:330—4.
[11] Tada A. 67Gallium whole body scintigraphy and single photon emission computed tomography (SPECT) in sarcoidosis. Nippon Rinsho 2002;60:1753—8 [in Japanese with English abstract].
[12] Yamagishi H, Shirai N, Takagi M, Yoshiyama M, Akioka K, Takeuchi K, et al. Identification of cardiac sarcoidosis with 13N-NH3/18F-FDG PET. J Nucl Med 2003;44:1030—6.
[13] Okumura W, Iwasaki T, Toyama T, Iso T, Arai M, Oriuchi N, et al. Usefulness of fasting 18F-FDG PET in identification of cardiac sarcoidosis. J Nucl Med 2004;45:1989—98.
[14] Wagner A, Mahrholdt H, Holly TA, Elliott MD, Regenfus M, Parker M, et al. Contrast-enhanced MRI and routine single photon emission computed tomography (SPECT) perfusion imaging for detection of subendocardial myocardial infarcts: an imaging study. Lancet 2003;361:374—9.
[15] Matoh F, Hayashi H, Terada H, Satoh H, Katoh H, Urushida T, et al. Usefulness of delayed enhancement magnetic resonance imaging for detecting cardiac rupture caused by small myocardial infarction in a case of cardiac tamponade. Circ J 2005;69:1556—9.
[16] Matoh F, Satoh H, Shiraki K, Urushida T, Katoh H, Takehara Y, et al. Usefulness of delayed enhancement magnetic resonance imaging to differentiate dilated phase of hypertrophic cardiomyopathy and dilated cardiomyopathy. J Cardiac Fail 2007;13:372—9.
[17] Riedy K, Fisher MR, Belic N, Koenigsberg D. MR images of myocardial sarcoidosis. Am J Roentgenol 1988;151:915—6.
[18] Chandra M, Siverman ME, Oshinski J, Pettigrew R. Diagnosis of cardiac sarcoidosis aided by MRI. Chest 1996;110:562—5.
[19] Shimada T, Shimada K, Sakane T, Ochiai K, Tsukihashi H, Fukui M, et al. Diagnosis of cardiac sarcoidosis and evaluation of effects of steroid therapy by gadolinium-

DTPA-enhanced magnetic resonance imaging. Am J Med 2001;110:520—7.
[20] Vignaux O, Dhote R, Duboc D, Blanche P, Dusser D, Waber S, et al. Clinical significance of myocardial magnetic resonance abnormalities in patients with sarcoidosis. A 1-year follow-up study. Chest 2002;122:1895—901.
[21] Paule P, Braem L, Heno P, Miltgen J, Verrot D, Fourcade L, et al. Diagnosis of cardiac sarcoidosis and follow-up of 24 consecutive patients. Rev Med Intern 2004;25:357—62.
[22] Dhote R, Vignaux O, Blanche P, Duboc D, Dusser D, Brezin A, et al. Value of MRI for the diagnosis of cardiac involvement in sarcoidosis. Rev Med Intern 2003;24:151—7.
[23] Vignaux O. Cardiac sarcoidosis: spectrum of MRI features. Am J Roentgenol 2005;184:249—54.
[24] Tadamura E, Yamamuro M, Kubo S, Kanao S, Saga T, Harada M, et al. Effectiveness of delayed enhanced MRI for identification of cardiac sarcoidosis: comparison with radionuclide imaging. Am J Roentgenol 2005;185:110—5.
[25] Smedema JP, Snoep G, Kroonenburgh MPG, Van Geuns RJ, Dassen WRM, Gorgels APM, et al. Evaluation of the accuracy of gadolinium-enhanced cardiovascular magnetic resonance in the diagnosis of cardiac sarcoidosis. J Am Coll Cardiol 2005;45:1683—90.
[26] Hiraga Y. Proposal by the Specific Diffuse Pulmonary Disease Research Group. Sarcoidosis Division by the Japanese Ministry of Health and Welfare; 1989. p. 13—6 [in Japanese].
[27] Hiraga H, Hiroe M, Iwai K, Guideline for dagnosis of cardiac sarcoidosis: study report on diffuse pulmonary diseases by the Japanese Ministry of Health and Welfare; 1993: p. 23—4 [in Japanese].
[28] Sugi T, Satoh H, Uehara A, Katoh H, Terada H, Matsunaga M, et al. Usefulness of stress myocardial perfusion imaging for evaluating asymptomatic patients after coronary stent implantation. Circ J 2004;68:462—6.
[29] Torizuka T, Nobezawa S, Momiki S, Kasamatsu N, Kanno T, Yoshikawa E, et al. Short dynamic FDG-PET imaging protocol for patients with lung cancer. Eur J Nucl Med 2000;27:1538—42.
[30] Berman DS, Kiat H, Friedman JD, Wang FP, Van Train K, Matzer L, et al. Separate acquisition rest thallium-201/stress technetium-99m sestamibi dual-isotope myocardial prefusion single-photon emission computed tomography: a clinical validation study. J Am Coll Cardiol 1993;22:1455—64.
[31] Lorell B, Aldeman EL, Mason JW. Cardiac sarcoidosis: diagnosis with endomyocardial biopsy and treatment with corticosteroids. Am J Cardiol 1978;42:143—6.
[32] Uemura A, Morimoto S, Hiramitsu S, Kato Y, Ito T, Hishida H. Histologic diagnostic rate of cardiac sarcoidosis: evaluation of endomyocardial biopsies. Am Heart J 1999;138: 299—302.
[33] Edelman R. Contrast-enhanced MR imaging of the heart: overview of the literature. Radiology 2004;232: 653—68.
[34] Moon JCC, McKenna WJ, McCrohon JA, Elliott PM, Smith GC, Pennell DJ. Toward clinical risk assessment in hypertrophic cardiomyopathy with gadolinium cardiovascular magnetic resonance. J Am Coll Cardiol 2003;41:1561—7.
[35] Takemura T. Epithelioid cell granuloma in sarcoidosis: light and electron microscopic morphology. Nippon Rinsho 2002;60:1704—13 [in Japanese with English abstract].
[36] Van Hoe L, Vanderhyden M. Ischemic cardiomyopathy: value of different MRI techniques for prediction of functional recovery after revascularization. Am J Roentgenol 2004;182:95—100.
[37] Line BR, Hunninghake GW, Keogh BA, Jones KA, Johnston GS, Crystal RG. Gallium-67 scanning to stage the alveolitis of sarcoidosis: correlation with clinical studies, pulmonary function studies, and bronchoalveolar lavage. Am Rev Respir Dis 1981;123:440—6.
[38] Leug AN, Brauner MW, Caillat-Vigneron N, Valeyre D, Grenier P. Sarcoidosis activity: correlation of HRCT findings with those of 67Ga scanning, bronchoalveolar lavage, and serum angiotensin-converting enzyme assay. J Comput Assist Tomogr 1998;22:229—34.
[39] Uemura A, Morimoto S. Cardiac sarcoidosis. Nippon Rinsho 2002;60:1794—800 [in Japanese with English abstract].
[40] Kim RJ, Chen EL, Lima JAC, Judd RM. Myocardial Gd-DTPA kinetics determine MRI contrast enhancement and reflect the extent and severity of myocardial injury after Acute reperfused infarction. Circulation 1996;94:3318—26.
[41] Flacke SJ, Fischer SE, Lorenz CH. Measurement of the gadopentetate dimeglumine partition coefficient in human myocardium in vivo: normal distribution and elevation in acute and chronic infarction. Radiology 2001;218:703—10.
[42] Tadamura E, Yamamuro M, Kubo S, Kanao S, Hosokawa R, Kimura T, et al. Multimodality imaging of cardiac sarcoidosis before and after steroid therapy. Circulation 2006;113:e771—3.